Automatic Self-Calibration of ARM Microwave Radiometers

J. C. Liljegren
Ames Laboratory
Ames, Iowa

Introduction

The Atmospheric Radiation Measurement (ARM) Program has deployed continuously operating Microwave Radiometers in remote locations including rural Oklahoma, islands in the tropical Pacific Ocean, and in northern Alaska. In order to assure that their calibrations are properly maintained, algorithms that permit the radiometer calibrations to be automatically and continuously updated have been developed and implemented.

Operation and Calibration Principles

The radiometer measures the equivalent blackbody brightness temperature, T_{sky} for each channel:

$$T_{sky} = T_{ref} + G\,(V_{sky} - V_{ref})\,f_w. \quad (1)$$

V_{sky} and V_{ref} are the signals measured when the radiometer is viewing the sky and reference blackbody target, respectively (see Figure 1). T_{ref} is the measured temperature of the reference target. The factor $f_w = 1/(1-\varepsilon)$ accounts for the polycarbonate foam window covering the mirror; ε is the window emissivity. G is the calibrated gain:

$$G = T_{nd} / (V_{ref+nd} - V_{ref}). \quad (2)$$

V_{ref+nd} is the signal when viewing the reference target with the noise diode energized. T_{nd} is the noise injection temperature determined from calibration. This is depicted graphically in Figure 2.

Tip Curves

An independent measurement of T_{sky} is needed to determine T_{nd}. For clear sky conditions, the optical thickness or opacity $\tau(\theta)$ at an elevation angle θ is given by

$$\tau(\theta) = \tau_{zen}\, m(\theta) \quad (3)$$

where τ_{zen} is the zenith opacity and m is the airmass: the ratio of the path length at θ to that at zenith. Using an estimated value of T_{nd}, values of T_{sky} are obtained for angles corresponding to m = 1 (zenith) and m = 1.5, 2, 2.5, and 3 on both sides of zenith. The opacities are calculated according to

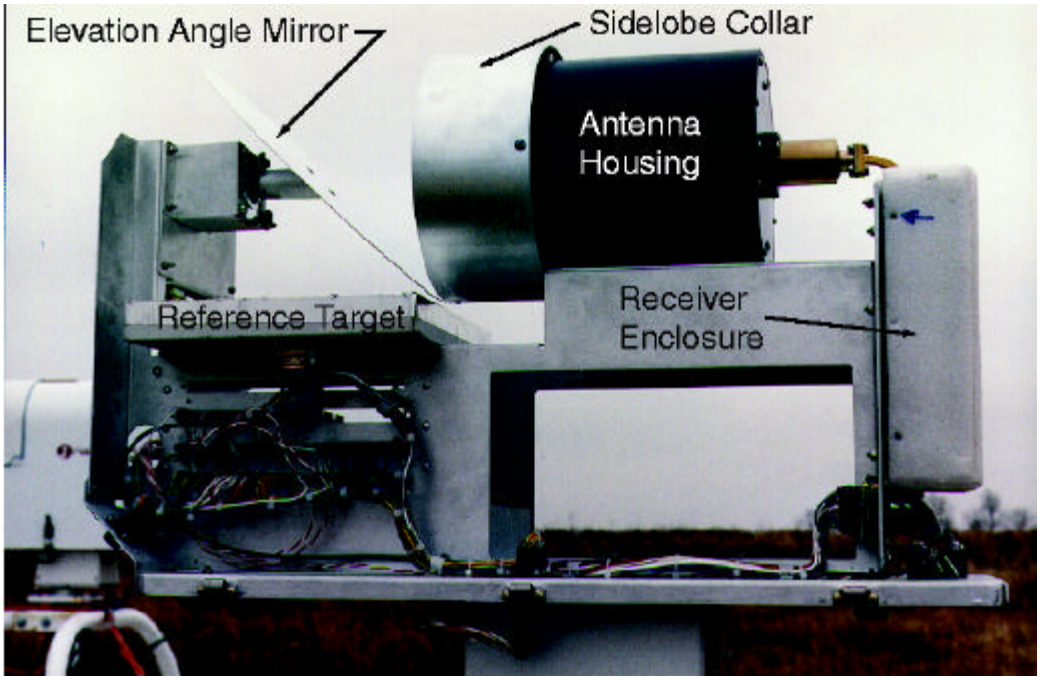

Figure 1. The Microwave Radiometer with its cover removed.

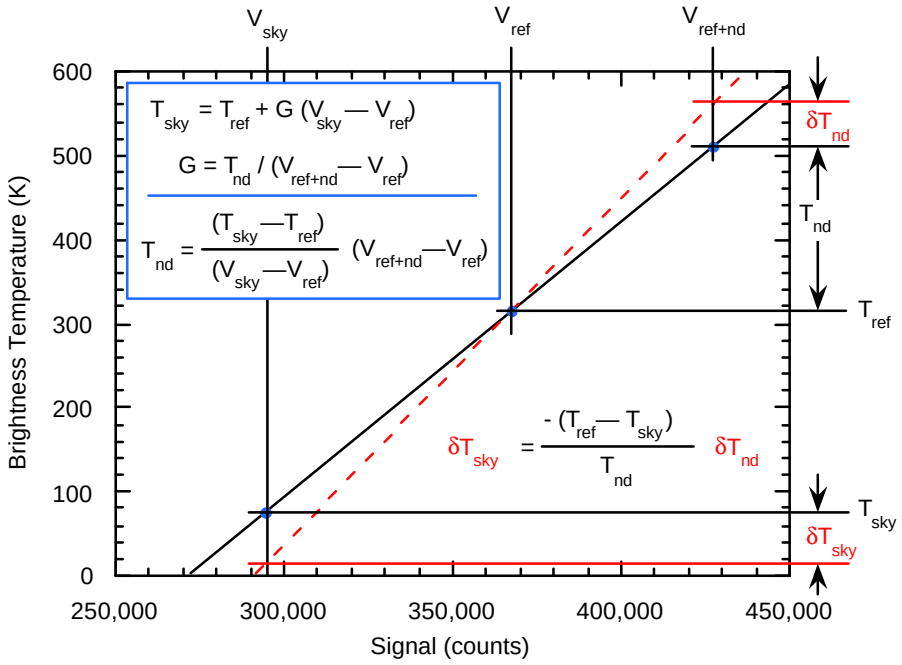

Figure 2. Schematic representation of radiometer measurement and calibration. The relationship between calibration and measurement errors is also illustrated.

$$\tau = \ln [(T_{mr} - T_{bg})/(T_{mr} - T_{sky})] \quad (4)$$

where T_{mr} is the atmospheric mean radiating temperature and T_{bg} is the cosmic background temperature (2.73 K). A linear regression of τ on m (i.e., a tip curve) is then calculated; the slope of the regression is an estimate of τ_{zen}. If the correlation coefficient R of the regression is at least 0.998, indicating that the sky is clear, then this estimate of τ_{zen} is used to estimate T_{sky}:

$$T_{sky} = T_{bg}\, e^{-\tau} + T_{mr}\,(1 - e^{-\tau}) \quad (5)$$

which, in turn, is used to improve the estimate of T_{nd}. This process is repeated with the new estimate of T_{nd} until the intercept of the regression converges to zero. (Normally only one iteration is needed.) The ARM Microwave Radiometers can acquire a tip curve in about 50 seconds.

Beam Correction

The antenna temperature T_{ant} measured by the radiometer represents a convolution of T_{sky} with the antenna power pattern. Because T_{sky} varies non-linearly with θ, T_{ant} is always greater than the value of T_{sky} at the beam center; the effective air mass m_{eff} is always greater than the actual value. To correct for this effect, the antenna was modeled as a circular aperture with a power pattern as shown in Figure 3a. The variation of T_{sky} with θ was modeled using Eqs. (3) and (5) except that the plane-parallel approximation ($m = 1/\sin\theta$) was replaced by the Niell wet mapping function. (Because $1/\sin\theta \rightarrow \infty$ as $\theta \rightarrow 0$, the plane-parallel assumption results in over-correction.) The resulting corrections are shown in Figure 3b.

Mirror Alignment

Due to continuous use, the mirrors on some of the radiometers have slipped slightly on their motor shafts. The resulting offset in elevation angle causes the tip curves to not pass the screening criterion ($R \geq 0.998$). To account for this, the offset is computed for the 31.4 GHz (liquid-sensitive) channel for each tip curve; each hour the median offset for the last 1000 tip curves is computed and the elevation mirror position is adjusted accordingly. The improvement arising from this adjustment is revealed in Figure 4.

In this figure are plotted differences in brightness temperatures for elevation angles corresponding to the same air mass but on opposite sides of zenith (e.g. 19.5° and 160.5° for m = 3). After this algorithm was installed, the bias in the clear-sky differences was reduced to zero; the correlation coefficient of the tip curve regressions increased to ≥ 0.999.

Automatic Calibration Algorithm

To assess whether the sky is sufficiently clear for calibration, a 30-minute running mean and standard deviation of liquid water path (LWP) are calculated. When the standard deviation falls below 0.008 mm

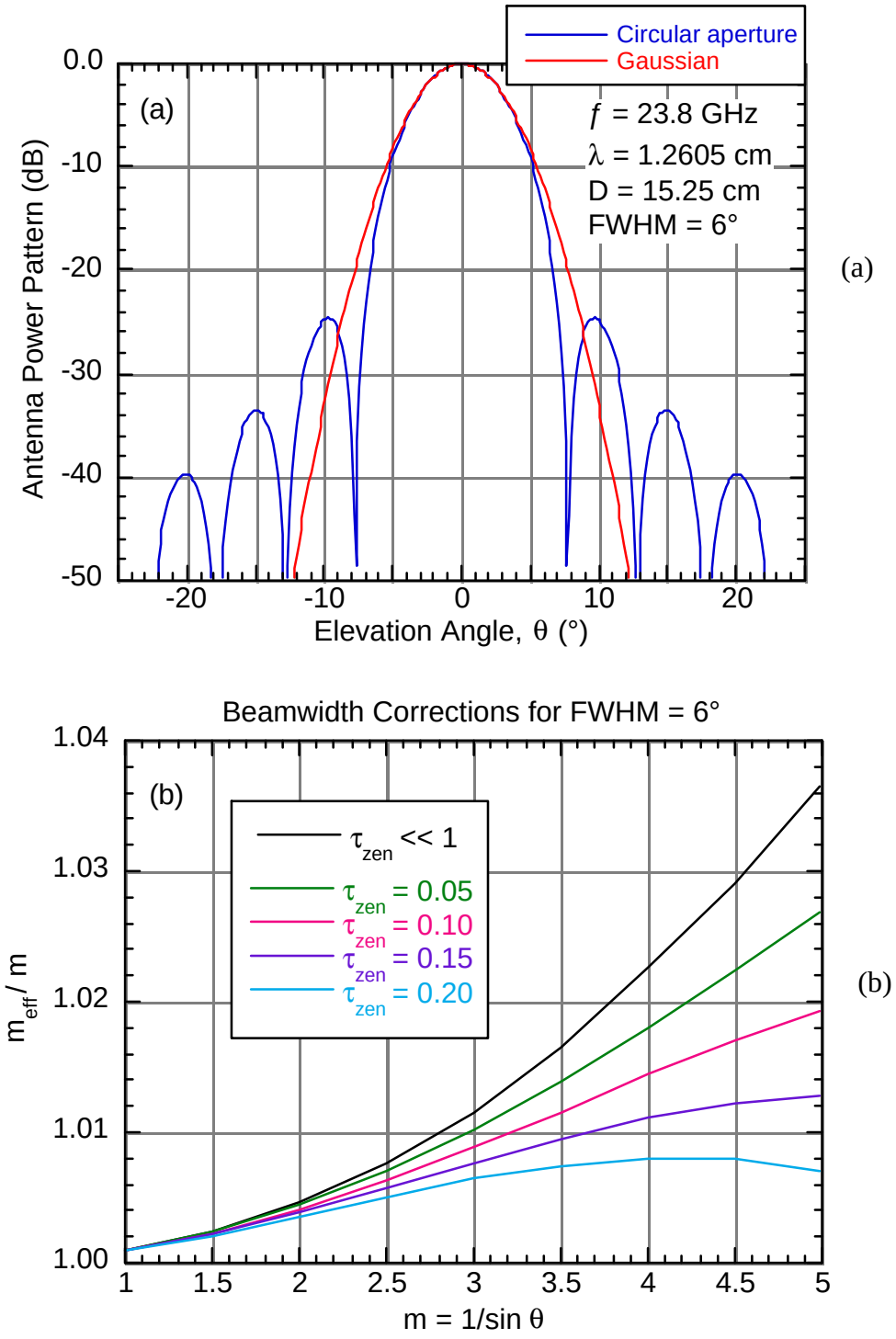

Figure 3. (a) Antenna power patterns: circular aperture (6" diameter) with parabolic amplitude taper (blue), equivalent Gaussian (red); (b) beam width corrections parameterized by zenith opacity.

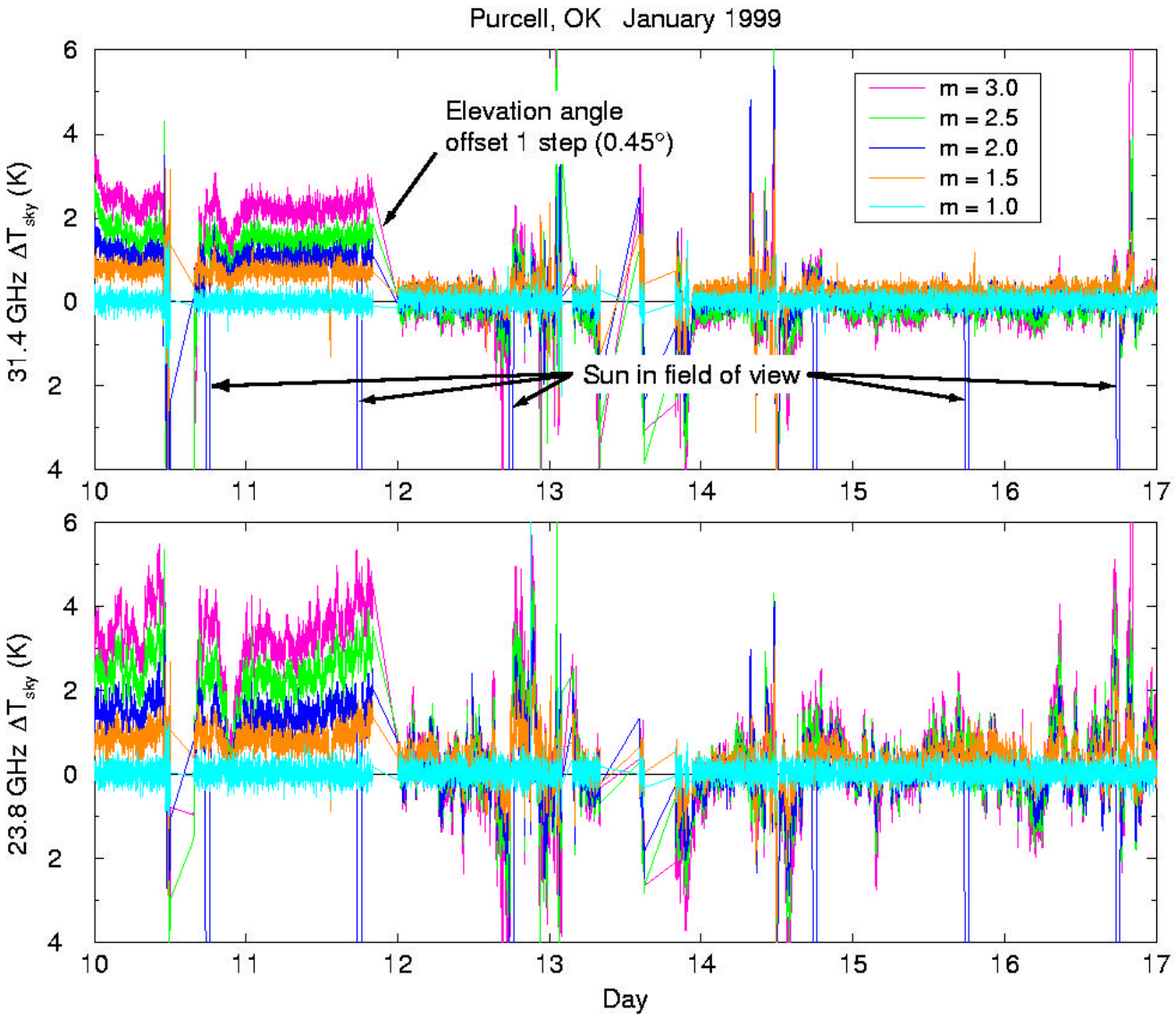

Figure 4. Differences in brightness temperatures for elevation angles on opposite sides of zenith having identical airmass values.

(2 x root mean square [rms] noise level), the radiometer begins acquiring tip curves. For each new instantaneous value of T_{nd}, a robust linear regression (least absolute deviation) of T_{nd} on T_{ref} is calculated using the most recent (up to 3000) values to continuously estimate $T_{nd,\,290}$ (the value of T_{nd} at T_{ref} = 290 K) and the temperature coefficient α. These are used to continuously predict T_{nd} from T_{ref}:

$$T_{nd} = T_{nd,\,290} + \alpha\,(T_{ref} - 290). \qquad (6)$$

Time series of T_{nd} are presented in Figure 5 for January 10-30, 1999. The value of T_{nd} predicted from T_{ref} tracks the 2-hour running median reasonably well, although apparently better at 23.8 GHz than at

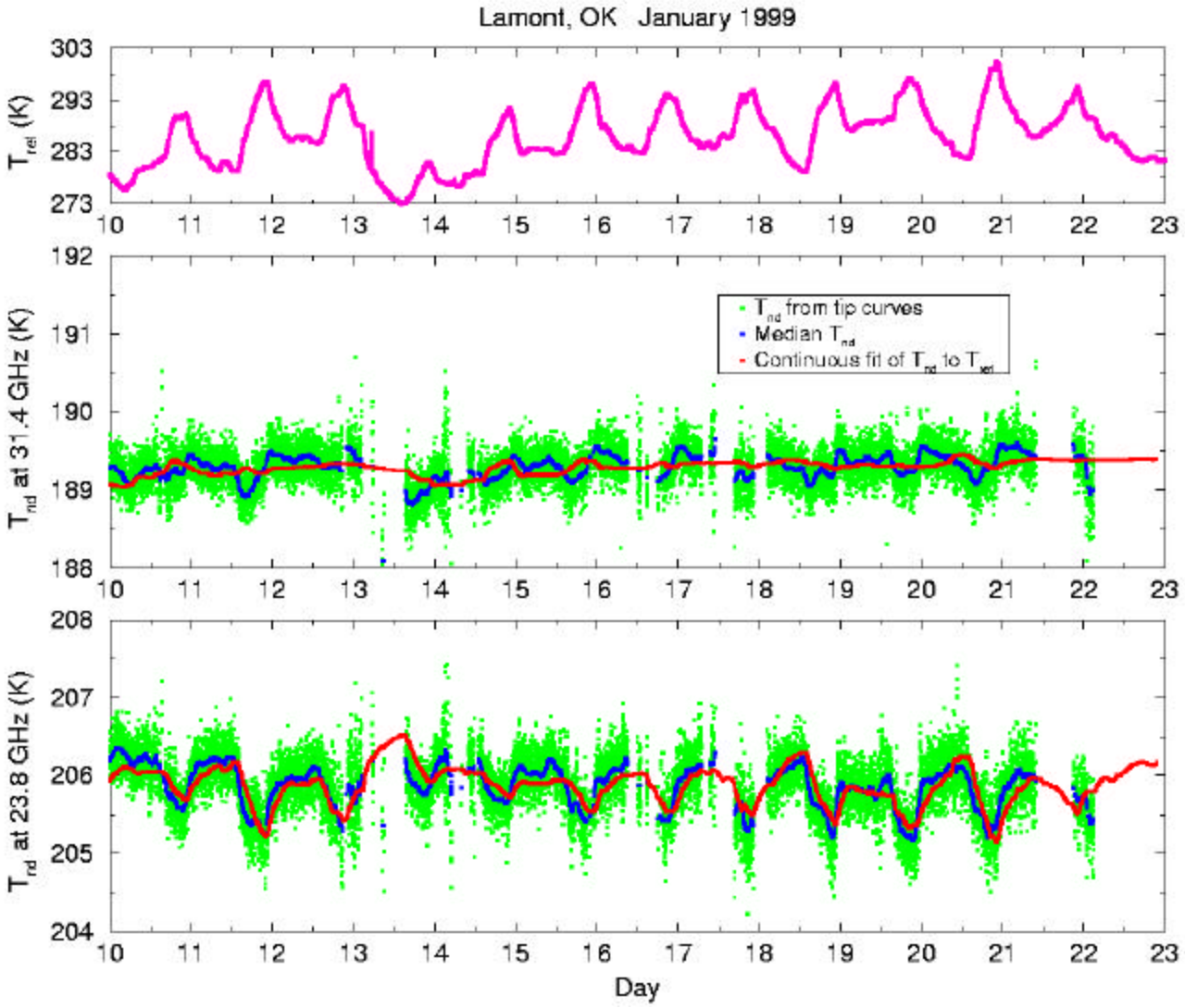

Figure 5. Time series of reference temperature T_{ref} (top panel). The middle and lower panels present time series of noise injection temperature T_{nd} from individual tip curves (green), a 2-hour running median (blue), and predicted from the continuous fit to T_{ref} (red) for the 31.4-GHz and 23.8-GHz channels, respectively.

31.4 GHz. The variations in T_{nd} at 31.4 GHz are considerably smaller and, as is apparent from the plots of T_{nd} vs. T_{ref} presented in Figure 6, the values of T_{nd} at 23.8 GHz exhibit a greater correlation with T_{ref}. In any case, the rms difference between the predicted values of T_{nd} and the running median is less than 0.2 K for both channels.

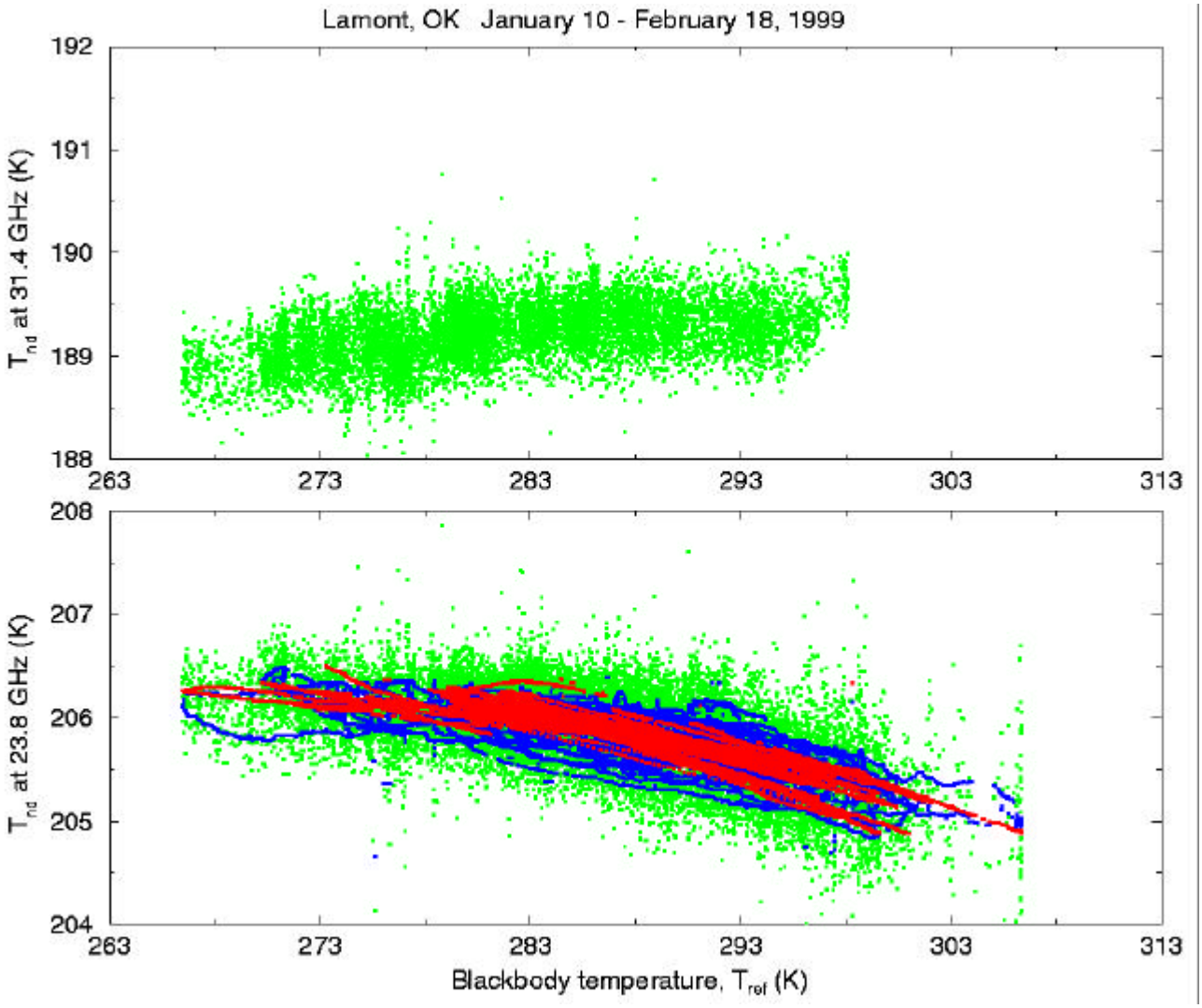

Figure 6. The correlation of T_{nd} with T_{ref} at 31.4 GHz (top panel) and 23.8 GHz (lower panel). For this instrument, the correlation is much stronger at 23.8 GHz than at 31.4 GHz. The values of T_{nd} predicted from T_{ref} agree with the median values to within 0.2 K rms.

Conclusions

A continuous, automatic self-calibration algorithm has been developed and implemented for ARM Microwave Radiometers that corrects for finite beam width effects, aligns/levels the elevation mirror and maintains the radiometer calibration to better than 0.2 K rms.